Ocean Systems Engineering, *Vol. 8, No. 2 (2018) 183-199*
DOI: https:// doi.org/10.12989/ose.2018.8.2.183

Numerical simulation of wave slamming on wedges and ship sections during water entry

Zhihua Ma and Ling Qian*

School of Computing, Mathematics & Digital Technology, Manchester Metropolitan University Manchester, M1 5GD, UK

(Received March 26, 2018, Revised June 8, 2018, Accepted June 10, 2018)

Abstract. The open source software OpenFOAM is utilised to simulate the water entry and hydrodynamic impact process of 2D wedges and ship hull sections. Incompressible multiphase flow solver interDyMFoam is employed to calculate the free fall of structure from air into water using dynamically deforming mesh technique. Both vertical and oblique entry of wedges of various dead-rise angles have been examined. A convergence study of dynamics as well as kinematics of the flow problem is carried out on successively refined meshes. Obtained results are presented and compared to the experimental measurements showing good agreement and reasonable mesh convergence of the solution.

Keywords: multiphase flow; free surface; wave impact

1. Introduction

Water wave impacting on ships is an important problem in naval engineering (Chuang 1970). Under rough sea states, the ship can be impinged by large waves at the bow. This causes the ship to experience large impact forces and high frequency vibrations with relatively long duration, and the violent pressure loadings can spread over the bow flare. The flare slamming phenomenon is usually accompanied by green water impact, in which a large amount of water breaks onto the ship deck and generates large pressures there (Xu and Duan 2009). Other types of hydrodynamic impacts including bottom slamming and wave slap can also occur under rough sea states.

Accurately predicting the impact loadings during these harsh events is of great importance to ship industry but it remains to be a big challenge to either theoretical analysis or experimental investigation due to the inherent strong nonlinearity of the problem (Faltinsen 2000). With the fast development of computer technology and numerical analysis, computational fluid dynamics (CFD) has been more frequently applied in various areas including aerospace engineering, bio-mechanics and chemistry, etc. There is also a continuous rise of the use of CFD as an important analysis and design tool in ship industry (Gu *et al.* 2014).

The present work evaluates the accuracy and capability of the open source CFD library OpenFOAM for the particular problem of water entry of wedges and ship hull sections based on the dynamics meshing approach. A selected cases from the drop tests carried out at Korea

*Corresponding author, Ph.D., E-mail: L.Qian@mmu.ac.uk

http://www.techno-press.org/?journal=ose&subpage=7 ISSN: 2093-6702 (Print), 2093-677X (Online)

Research Institute of Ships & Ocean Engineering (Hong *et al.* 2017) will be reproduced numerically and results compared with the experimental measurements. We use the dynamic deforming mesh technique to simulate the free fall of the structure from air into water. An incompressible multiphase interDyMFoam is employed to calculate the pressure and force loadings on the structure. Mesh convergence study is also carried out on successively refined meshes.

The remainder of the paper is organized as follows. The mathematical model and numerical solution schemes are firstly presented, which is followed by the detailed setup and test conditions of the water entry problems. The numerical results and discussions are then presented. Finally, conclusions from the current work are drawn.

2. Numerical model

The numerical method adopted in this work employs a cell centred, collocated finite volume scheme implemented in the open source CFD library OpenFOAM. This library provides multiple options of flow models including single- and multi-phase incompressible and compressible flows, different solution schemes like explicit and implicit time advancing methods. The use as well as further development of this CFD software has become more and more popular in recent years (Ma *et al*. 2016, Martínez Ferrer *et al*. 2016).

To deal with the free surface flows and the motion of falling objects, we utilise an incompressible multiphase flow solver interDyMFoam, which combine the underlying multiphase flow solver interFoam with dynamic deforming mesh techniques. This solver has the capability to deal with the 6DoF motion of moving objects. At the beginning, a suitable body-fitted mesh is generated to cover the whole flow domain. During the simulation, the mesh is dynamically deformed to accommodate the motion of the structure. For small amplitude motion, dynamic mesh could effectively handle the moving structure. The multiphase flow solver interFoam builds on the conservation law of mass, momentum as well the transport of volume fraction. It treats water and air as incompressible fluids with constant densities. It adopts pressure-based methods (PISO) to solve the multiphase flows. For completeness of description, the mathematical equations of the underlying flow solver interFoam are given as follows. .

The mass conservation equation is given by

$$\frac{\partial \rho}{\partial t} + \nabla \cdot (\rho \mathbf{U}) = 0 \tag{1}$$

in which ρ is the density of water-air mixture, $\mathbf{U}$ the velocity vector. The momentum equation is given by

$$\frac{\partial \rho \mathbf{U}}{\partial t} + \nabla \cdot (\rho \mathbf{U}\mathbf{U}) - \nabla \cdot (\mu \nabla \mathbf{U}) = \sigma \kappa \nabla \alpha - \mathbf{g} \cdot \mathbf{x}\, \nabla \rho - \nabla p_{\mathrm{d}}, \tag{2}$$

where σ is the surface tension coefficient; the curvature of the interface is calculated as $\kappa = \nabla \cdot (\nabla \alpha / |\nabla \alpha|)$; $p_{\mathrm{d}} = p - \rho \mathbf{g} \cdot \mathbf{x}$ is the dynamic pressure; $\mathbf{g}$ is the gravitational acceleration and $\mathbf{x}$ is the position vector. A transport equation for the water volume fraction used to capture the free surface is given by

$$\frac{\partial \alpha}{\partial t} + \mathbf{U} \cdot \nabla \alpha + \nabla \cdot \mathbf{U}_{\mathrm{c}} \alpha (1 - \alpha) = 0 \tag{3}$$

where $\alpha = \Omega_{\text{water}}/(\Omega_{\text{water}} + \Omega_{\text{air}})$ is the volume fraction for the water component, $\nabla \cdot \mathbf{U}_c\alpha(1-\alpha)$ is an anti-diffusion term utilized to sharpen the interface. The mixture density is calculated by

$$\rho = \alpha\rho_{\text{water}} + (1-\alpha)\,\rho_{\text{air}} \tag{4}$$

in which the two constants ρ_{water} and ρ_{air} are densities of water and air respectively. Eqs. (1) to (4) are solved in an iterative way by using the PISO method, of which the key steps are listed as follows

1) Solve the volume fraction transport Eq. (3).
2) Update the mixture density according to Eq. (4).
3) Solve the momentum Eq. (2).
4) Solve the pressure correction equation.

When the mesh is moving or deforming a relative velocity, from which the velocity of a mesh face is subtracted, should be used for calculating the convective flux. Readers may refer to a recent work of the authors (Ma *et al*. 2016) for more details of the mathematical equations as well as the solution procedures of the flow solver.

3. Drop test setup

Fig. 1 shows the geometry of 2D wedges. The length and width of the wedges are 600 mm and 800 mm respectively. The deadrise angles of the wedges are either 20 or 30 degrees. In the experiments, the wedges are attached to a guide rail and are allowed to fall freely in the vertical direction from different heights. The wedges may have zero or non-zero tilting angles. Table 1 lists the test conditions of the 2D wedges. Two pressure transducers and two local force sensors are installed on the wedges. Near the bottom end of the guide rail, a stiff spring is installed there to decelerate the test object in order to prevent it from hitting the bottom of the water tank. In the present numerical study we calculate three cases for the wedges, but the spring device is not included.

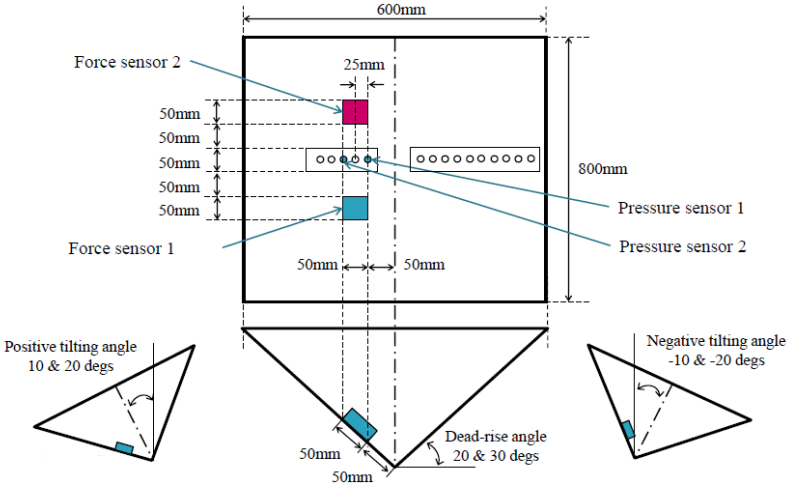

Fig. 1 The geometry of the wedges

Table 1 Test matrix of 2D wedge drop test

Test ID	Dead-rise angle	Tilting angle (deg)	Drop height (m)
01	30	0	0.5
05	30	20	0.5
08	20	0	0.25

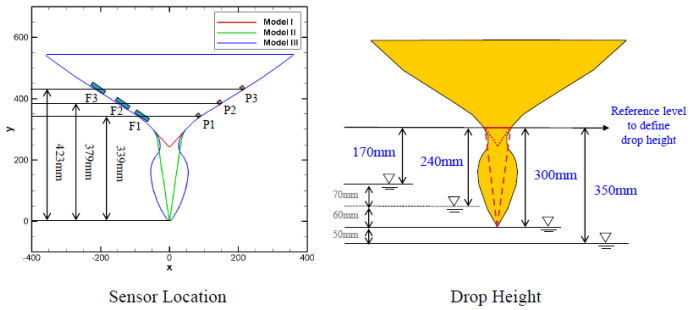

Fig. 2 The geometry of the ship sections

Fig. 2 shows the geometry of ship hull sections. In the experiments there are three different configurations of the models. Three pressure transducers and three local force sensors are installed on the models. In the present study, only the test case number 11 for model III with a drop height of 300 mm will be considered.

4. Results and discussions

4.1 Mesh generation and refinement

The meshing tool, blockMesh, of OpenFOAM only provides basic features and is not straightforward to use. Therefore, we use another open-source meshing tool, Gmsh, for mesh generation in all test tests. Gmsh provides a GUI as well as parametric script files to users. It can generate unstructured, structured and hybrid 2D/3D meshes. If the geometry has minor changes such as an increase/decrease of the deadrise angle by a few degrees, a new suitable mesh could be easily generated by applying minor changes to the parametric script file. In the present work, we generate a 2D structured mesh covering a rectangular domain of 4 m long and 4 m high. The water depth is set to 2 m. The generated mesh is converted to the format of OpenFOAM by using the tool gmshToFoam. The left, right and bottom boundaries are treated as solid walls; the top boundary is treated as an open boundary with zero gradient in velocity and constant total pressure. The motion of the test object is constrained to 1DoF in the vertical direction only. Table 2 lists the number of mesh cells for each of the wedge test cases. A relatively coarse mesh (A) is firstly generated by Gmsh, then the mesh resolution is doubled in both x and y directions by using the

meshing tool refineMesh in OpenFOAM and so we can obtain a relatively fine mesh (B). The mesh is then refined again in both *x* and *y* directions to obtain the finest mesh (C).

Table 2 Number of mesh cells for wedge test cases

Test ID	Mesh A	Mesh B	Mesh C
01	24000	96000	384000
05	24000	96000	384000
08	21600	86400	345600

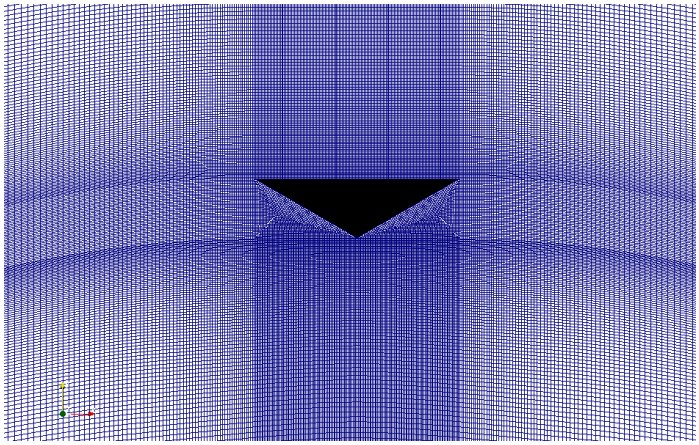

Fig. 3 A pre-deformed mesh at t=0 for test case 01. The wedge is pre-moved in the positive y direction by 0.3 m

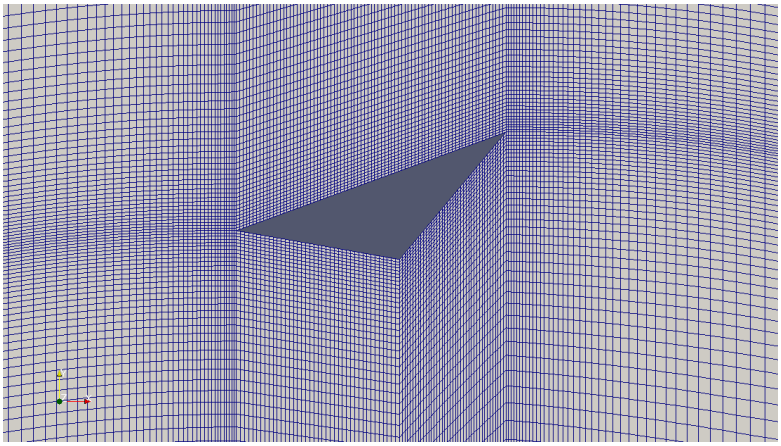

Fig. 4 A pre-deformed mesh at t=0 for test case 05

4.2 Dynamically deforming mesh

To handle moving boundaries with body-fitted mesh methods, there are generally two options. One is the overset grid method and the other is the dynamically deforming mesh method. OpenFOAM adopts the latter, which moves the mesh points at every time step during the motion of the body. Usually the mesh points attached to the body have the largest motion, and the largest mesh motion from the solid body is proportionally distributed on the whole domain in order to have a high-quality mesh. There are several techniques available to move the mesh in OpenFOAM. These include Laplacian smoother, solid body rotation stress (SBRStress) equation solver and radial basis function (RBF) interpolation (Bos 2010). We select the sixDoFRigidBodyMotion solver in OpenFOAM 2.3.0, and this solver exclusively uses the RBF method to smooth out the mesh motion.

Compared to the overset meshing which needs to process multiple meshes at every time step including hole cutting and data interpolation, the dynamic mesh method is relatively simple and efficient as it focuses on a single mesh. However, the dynamic deforming mesh method has limited capability to deal with large displacement and/or rotational motion of bodies. Excessive body motion may deteriorate the mesh quality and lead to the crash of the flow solver. The sixDoFRigidBodyMotion solver in OpenFOAM 2.3.0 has no capability to re-generate a mesh during the simulation, and this hinders the use of it to deal with large amplitude of body motions.

The two tests 01 and 05 have the same relatively large drop height 0.5 m compared to the size of the wedges. A simple use of the mesh generated by Gmsh for these three cases from the start will easily lead to the crash of the flow solver. To circumvent this difficulty, we pre-deform the mesh in the positive vertical direction by moving the wedges with a proper distance saying 0.2 m or 0.3 m. Fig. 3 gives an example of the pre-deformed mesh for test case 01. Fig. 4 exhibits the pre-deformed mesh for test case 05. The drop height for wedge test case 08 is only 0.25 m, we found that it is not necessary to pre-deform the mesh, and so we directly use the mesh generated by Gmsh. For ship section case 11 we pre-deform the mesh by moving the structure by 0.3 m upwards as shown in Fig. 5.

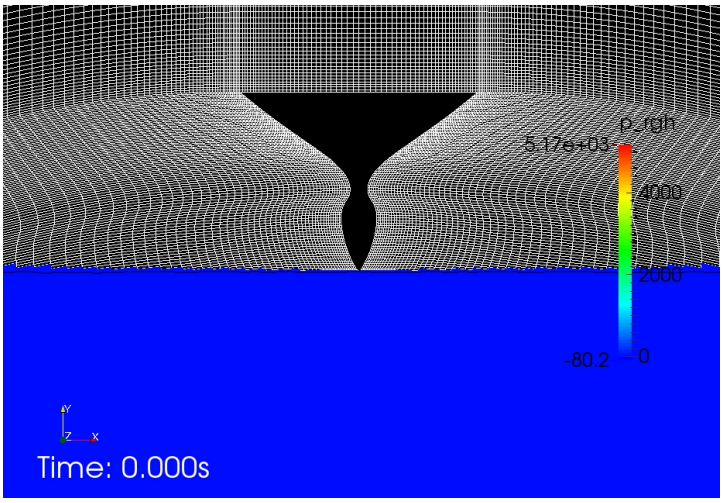

Fig. 5 The pre-deformed mesh at t=0 for ship section case 11

4.3 Time step and CPU time

The choice of time step has large influence on the solution stability and temporal/spatial accuracy. For all the test cases considered in the present work, we firstly tried a fixed time step of 1 ms.

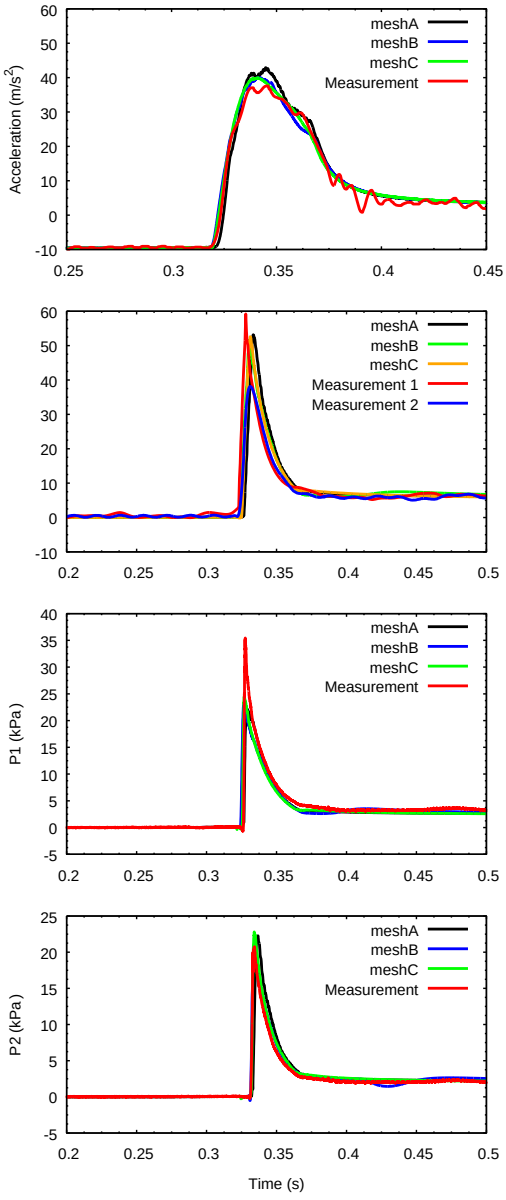

Fig. 6 Computed and measured acceleration, force and local pressures for 2D wedge test 01. Measurements 1 and 2 represent the readings of force sensors 1 and 2

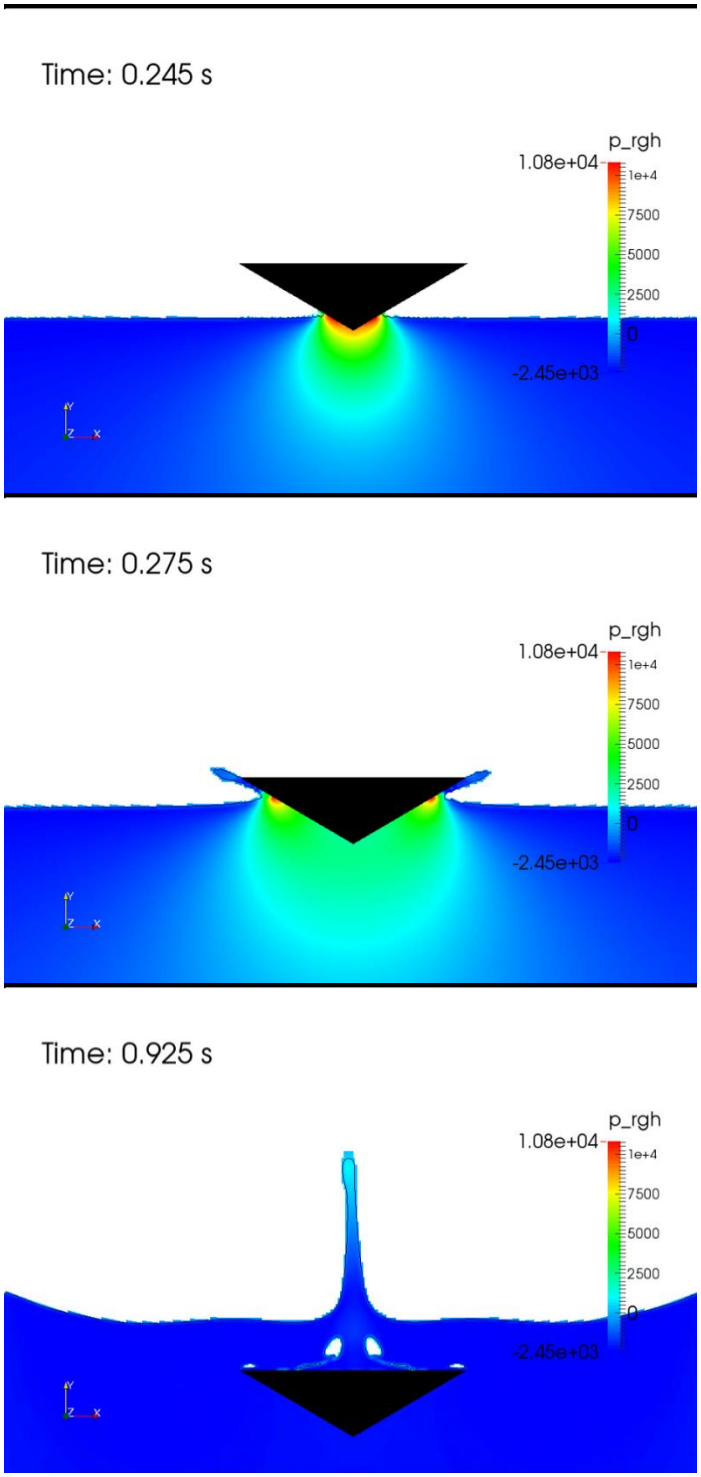

Fig. 7 Snapshots of the computed free surface and dynamic pressure contours for 2D wedge test 01

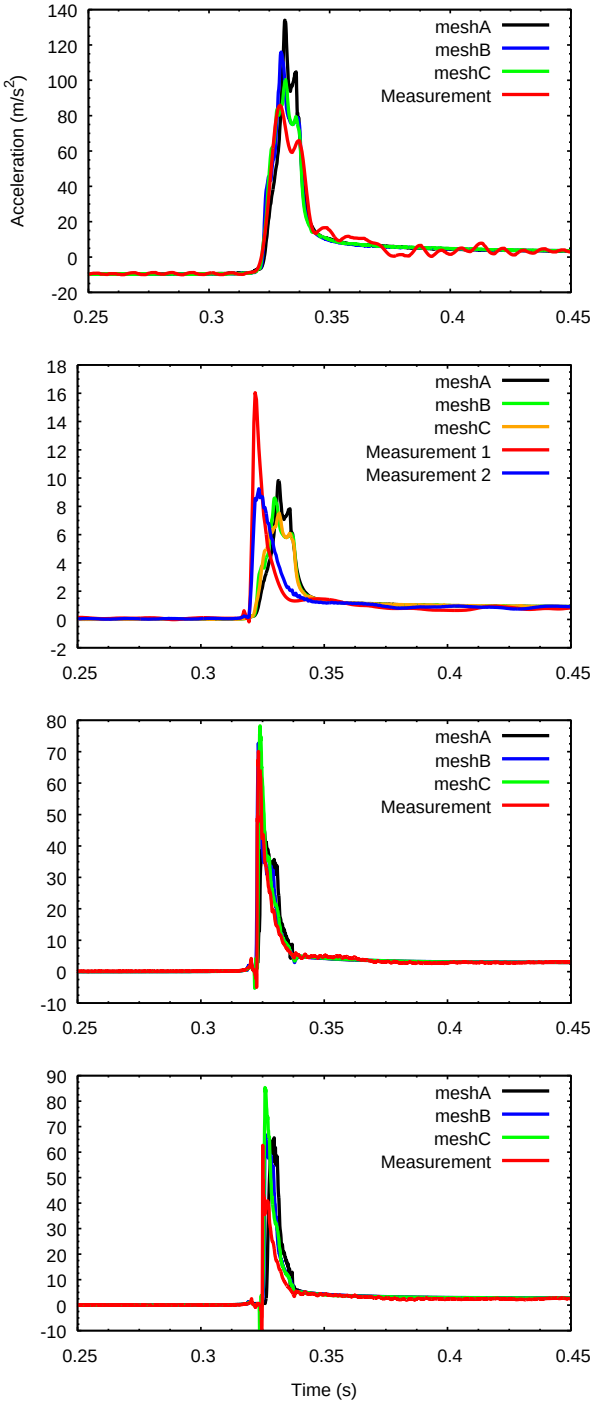

Fig. 8 Computed and measured acceleration, force and local pressures for 2D wedge test 05. Measurements 1 and 2 represent the readings of force sensors 1 and 2

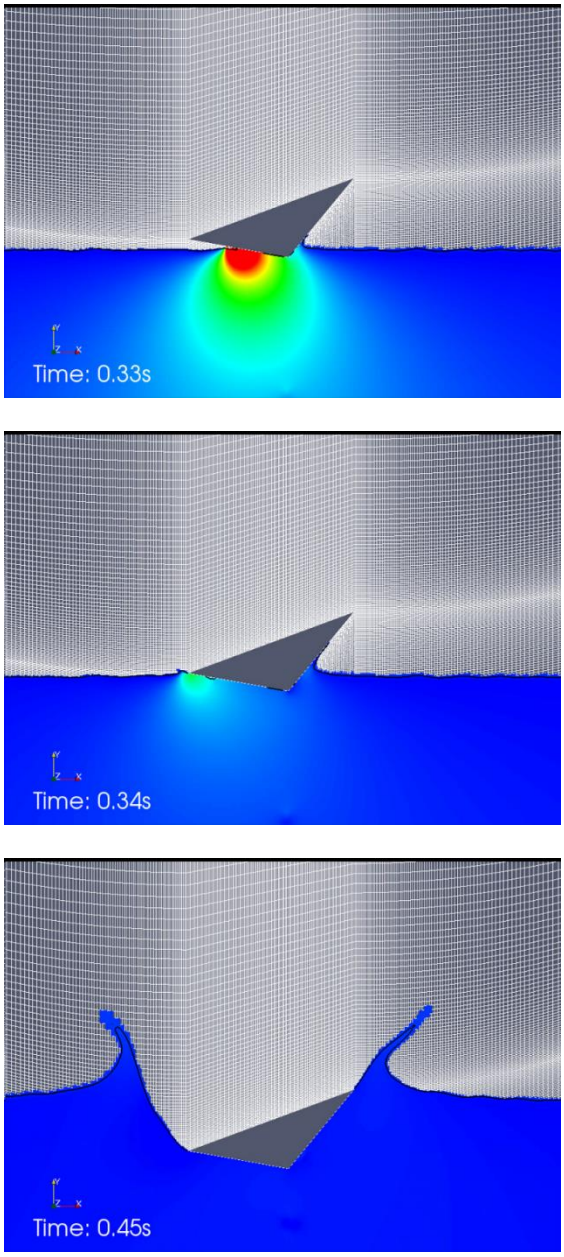

Fig. 9 Snapshots of the computed free surface and dynamic pressure contours for 2D wedge test 05

The solution procedure was stable but the obtained results have large discrepancies with the experimental data. Then we reduced the time step to 0.1 ms for all the test cases and the obtained numerical solutions including pressures, force and acceleration were greatly improved. To complete a one-second physical time simulation, it took us about 40 minutes using 8 CPU cores for the coarsest level of mesh. The CPU (wall) time cost will be increased by a factor of 4 when using a mesh refined in both x and y directions if the time step is fixed.

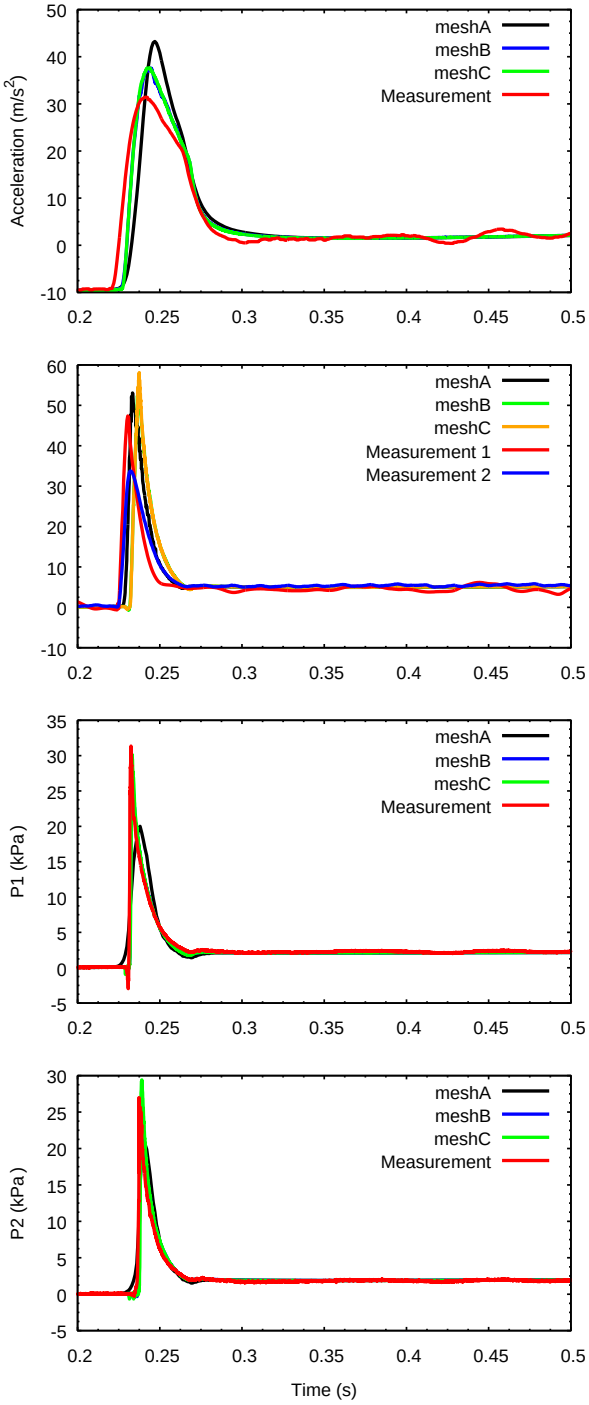

Fig. 10 Computed and measured acceleration, force and local pressures for 2D wedge test 08. Measurements 1 and 2 represent the readings of load cells 1 and 2

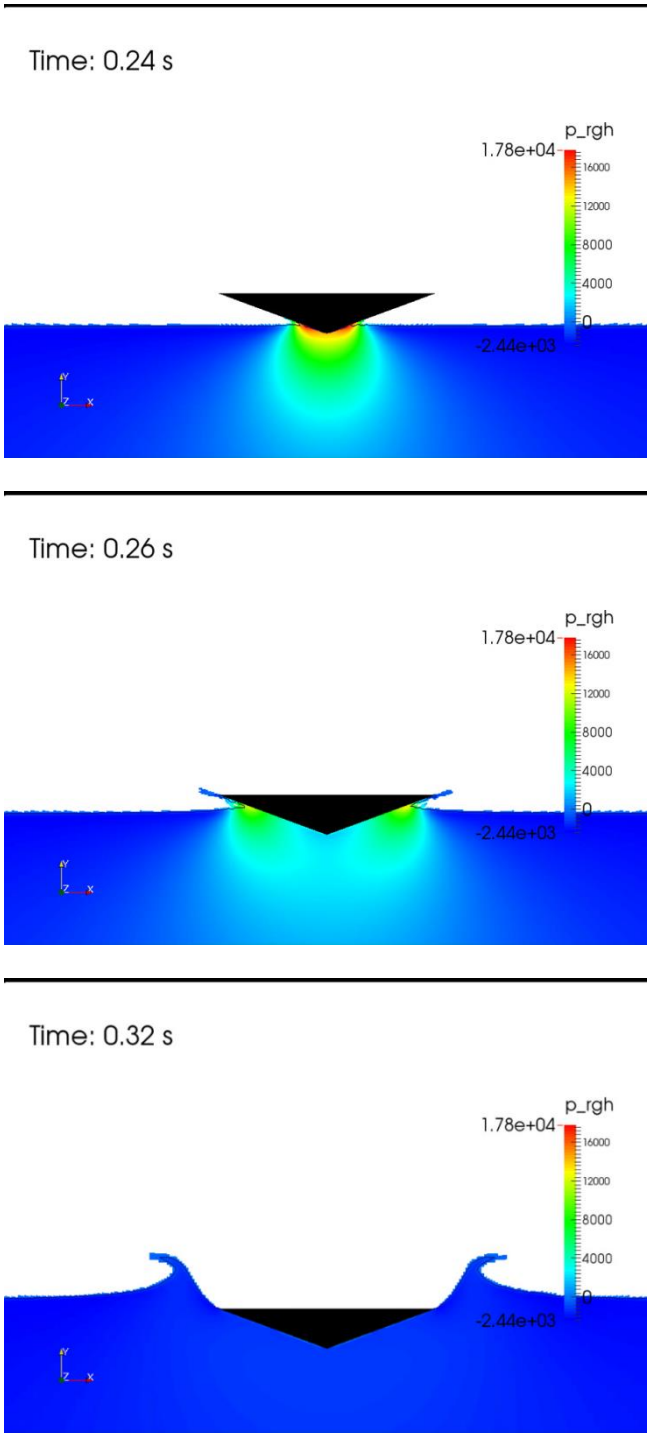

Fig. 11 Snapshots of the computed free surface and dynamic pressure contours for 2D wedge test 08

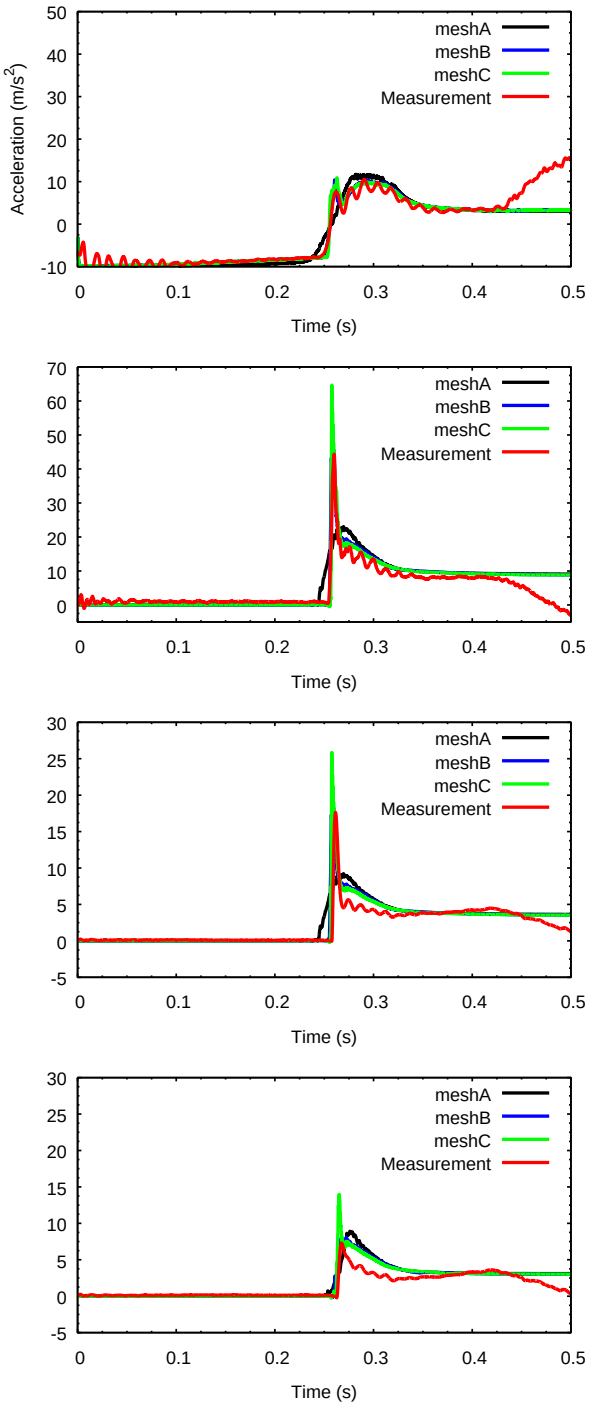

Fig. 12 Computed and measured acceleration, local forces and pressures for ship section test 11

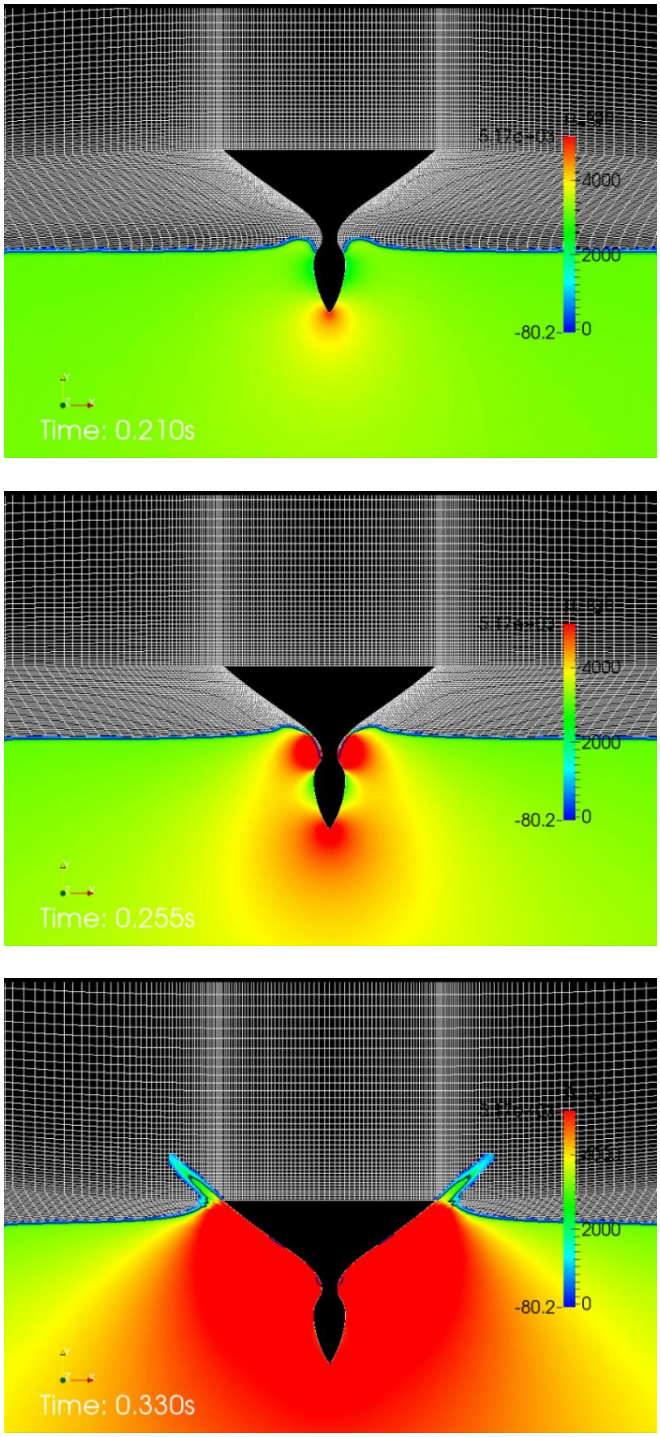

Fig. 13 Snapshots of the computed free surface and dynamic pressure contours for ship section test 11

4.4 Wedge test 01

Fig. 6 shows the measured and computed acceleration, force as well as local pressures for the 2D wedge test 01. The computed results are generally in a reasonable agreement with the experimental measurements. Considering the acceleration, the numerical mesh converged result is a bit higher than the measurement, but the trend is in a good agreement. Looking at the local impact force, the computed peak value is around 52 N, force sensor 1 gives the peak reading of 60 N and force sensor 2 gets the peak vale of 38 N. At P1 there is a big discrepancy between the computation and measurement. The numerical mesh converged solution gives a peak value of 25 kPa and the measured maximum pressure is near 35 kPa. At P2 the computation and measurement are much closer, of which the peak values are between 20 kPa and 23 kPa. According to similarity solution for wedge slamming problems P1 and P2, which are close to each other, should have similar peak impact pressures. The computed peak values at these two points are close each other within 23 kPa and 25 kPa. It seems that the pressure measured at P1 is a bit suspicious. Despite the different peak values, the computed durations of pressure spikes at P1 and P2 compare well with the experiment measurements. Fig. 7 shows several snapshots of the computed free surface and dynamic impact pressure at t=0.245, 0.275 and 0.925 s. It is clearly shown that high pressure builds up at the wedge tip and moves upwards along the wedge surface. The flow is symmetric at early stages, however it becomes asymmetric at t=0.925 s.

4.5 Wedge test 05

Fig. 8 shows the measured and computed acceleration, force as well as local pressures for the 2D wedge test 05. The computation for this case becomes difficult due to the large titling angle. The phases of computed acceleration agree well with experiment measurements, but the mesh convergence of the peak values especially the first peak is problematic. The similar problem could be seen for local force computation, while an even big discrepancy between the simulation and measurement could be spotted for the phase. The rise time of the computed force spike is much longer than experimental measurements. The peak pressures computed at P1 and P2 are around 78 kPa and 84 kPa. The measured peak pressure is 70 kPa at P1 and 62 kPa at P2. Fig. 9 shows several snapshots of computed free surface and dynamic impact pressure.

4.6 Wedge test 08

Fig. 10 shows the measured and computed acceleration, force as well as local pressures for the 2D wedge test 08. The mesh converged acceleration is a bit higher than the measured data by 8 m/s^2 considering the peak value. The mesh converged peak local force is around 53 N, force sensor 1 gives a reading of 48 N and force sensor 2 gives a reading of 33 N. The computed peak pressures at P1 and P2 are 30 kPa and 29 kPa. The measured peak pressure is 32 kPa at P1 and 27 kPa at P2. Figure 11 shows several snapshots of the computed free surface and dynamic impact pressure at t=0.24, 0.26 and 0.32 s.

4.7 Ship section test 11

Fig. 12 shows the measured and computed acceleration, force as well as local pressures for the ship section test 11. The computed results are generally in a reasonable agreement with the

experimental measurements. The first peak of mesh converged acceleration is around 11 m/s^2, the experimental result is about 8 m/s^2. After the first acceleration spike, the measured acceleration keeps pulsating due to the expansion and contraction of two trapped air pockets. The phenomenon could not be successfully captured by the incompressible solver adopted in the present work. The peak value of mesh converged local force at F1 is about 65 N, and the measured peak value is around 45 N. The computed maximum pressure is around 27 kPa at P1 and 18 kPa at P2. The measured results are 17 kPa and 7 kPa at P1 and P2 respectively. Fig. 13 shows several snapshots of the computed free surface and dynamic impact pressure. It can be seen that OpenFOAM cannot successfully capture the two large air pockets, which are clearly observed in experiments.

5. Conclusions

A numerical simulation was carried out to investigate the water entry of 2D wedges and ship sections. The open source CFD library OpenFOAM is utilised to simulate the hydrodynamic impact process. Convergence study is carried out on successively refined meshes. The computed impact loadings show reasonable mesh convergence and compare well with experimental measurements. This validates the use of OpenFOAM for hydrodynamic slamming problems.

Through this study we have noticed some issues of this open source CFD library, to which attention should also be paid by the community. The component solver interFoam employs the anti-diffusion term in the volume fraction transport equation to sharpen the free surface. It helps to improve the accuracy and convergence rate of the numerical method indeed. However, this term is purely constructed in a mathematical way without physical considerations. In fact this could cause asymmetry in the solution for a symmetric flow problem even when symmetric conditions and meshes are used (Martínez Ferrer *et al.* 2016).

Dynamic deforming mesh is a good and economic approach for modelling moving bodies with small amplitude motions since mesh re-generation is not necessary. However, it is not effective for moving bodies with large amplitude motions, which could distort the mesh and crash the computation. Global or local re-generation of the deforming mesh, which could be a favorable option to cure the problem, is not presently provided in OpenFOAM. In addition the solver interDyMFoam could be ten times slower than interFoam due to the use of dynamic mesh. OpenFOAM uses RBF method to solve the motion of the dynamic mesh. This method could provide relatively smooth mesh but is quite slow. The low efficiency of the dynamic mesh solver brings quite a big penalty to not only serial single-core computation but also parallel computing using MPI on multi-node clusters.

Acknowledgements

This research was supported by the Engineering and Physical Sciences Research Council (EPSRC), U.K. Project: A Zonal CFD Approach for Fully Nonlinear Simulations of Two Vessels in Launch and Recovery Operations, under Grant No. EP/N008839/1. The authors would also like to express gratitude to the Korea Research Institute of Ships & Ocean Engineering for providing the experimental data.

References

Chuang, S.L. (1970), "Investigation of impact of rigid and elastic bodies with water", Tech. Rep. No. NSRDC-3248 (Department of the Navy, Washington, D. C. 2000).

Faltinsen, O. (2000). "Hydroelastic slamming", *J. Mar. Sci. Technol*., **5**, 49-65.

Frank Martijn, B.O.S. (2010), "Numerical simulations of flapping foil and wing aerodynamics: Mesh deformation using radial basis functions", PhD Thesis, Delft University of Technology, Netherland.

Gu, H., Qian, L., Causon, D., Mingham, C. and Lin, P. (2014), "Numerical simulation of water impact of solid bodies with vertical and oblique entries", *Ocean Eng*., **75**, 128-137.

Hong, S.Y., Kim, K.H and Hwang, S.C. (2017), "Comparative study of water-impact problem for ship section and wedge drops", *Int. J. Offshore Polar.*, **27**(2), 123-134.

Kim, K.H., Lee, D.Y., Hong, S.Y., Kim, B.W., Kim, Y.S. and Nam, B.W. (2014), "Experimental study on the water impact load on symmetric and asymmetric wedges", *Proceedings of the 24th International Ocean and Polar Engineering Conference*, Busan, Korea, Juan 15-20.

Ma, Z., Causon, D., Qian, L., Mingham, C. and Martínez Ferrer, P. (2016). "Numerical investigation of air enclosed wave impacts in a depressurized tank", *Ocean Eng*., **123**, 15-27.

Martínez Ferrer, P., Causon, D., Qian, L., Mingham, C. and Ma, Z. (2016), "A multi-region coupling scheme for compressible and incompressible flow solvers for two-phase flow in a numerical wave tank", *Comput. Fluids*, **125**, 116-129.

Qian, L., Causon, D.M., Mingham, C.G. and Ingram, D.M. (2006). "A free-surface capturing method for two fluid flows with moving bodies", *Proceedings of the Roy. Soc.: A*, **462**(2065), 21-42.

Southall, N., Choi, S., Lee, Y., Hong, C., Hirdaris, S. and White, N. (2015), "Impact analysis using CFD – A comparative study", *Proceedings of the 25th International Ocean and Polar Engineering Conference*, Kona, Big Island, Hawaii, USA, Juan 21-26.

Xu, G.D. and Duan, W.Y. (2009), "Review of prediction techniques on hydrodynamic impact of ships", *J. Mar. Sci. Appl.*, **8**, 204-210.

QM